UNIVERSITY OF CALIFORNIA SAN DIEGO

Non-spherical Cavitation in Soft Materials

A Thesis submitted in partial satisfaction of the requirements
for the degree Master of Science

in

Engineering Sciences (Mechanical Engineering)

by

Shuai Wu

Committee in charge:

Professor Shengqiang Cai, Chair
Professor Vitali F. Nesterenko
Professor Michael T. Tolley

2018

The Thesis of Shuai Wu is approved and it is acceptable in quality and form for publication on microfilm and electronically:

_____

_____

_____

Chair

University of California San Diego

2018

TABLE OF CONTENTS

LIST OF FIGURES

ACKNOWLEDGEMENTS

I would like to thank professor Shengqiang Cai first as work in this thesis was supported by him. I really appreciate the opportunity to do research in his group, where I learn a lot from this project. Also, professor Cai has an amazingly accurate sense and always provides me with brilliant ideas, which inspires me a lot during this work.

I would like to thank Professor Alfred Crosby in the University of Massachusetts Amherst for the experiment works, which gave me some ideas about our numerical analysis. Also, Yue Zheng provided me great suggestions for both thesis project and master study and I am really gratitude to her kind help.

Lastly, I would thank my parents and elder brother who give me great supports during my master study. It is their generous help that gives me the opportunity to do research in UCSD.

ABSTRACT OF THE THESIS

Non-spherical Cavitation in Soft Materials

by

Shuai Wu

Master of Science in Engineering Sciences (Mechanical Engineering)

University of California San Diego, 2018

Professor Shengqiang Cai, Chair

Cavitation in soft solid is a phenomenon that cavity in an elastomer can expand rapidly when inner pressure reaches a critical value. Most of previous study focus on expansion of spherical void within a soft solid. In this thesis, we consider the mechanical response of non-spherical cavity to inner pressure. First, ellipsoidal cavitation with various geometries from oblate one to prolate one is studied. It shows that prolate cavity needs higher asymptotic pressure than oblate one and spherical one has intermediate asymptotic pressure. Then needle induced tubular cavitation is studied from several aspects. We found needle retraction will decrease the critical pressure, and surface tension will increase the critical pressure. Also, localized bulging of tubular cavity happens at the defect when surface tension is large enough. We also study the debonding between soft solid and rigid needle. It is fast for elastomer and needle to debond when pressure is close to the critical pressure, but if volume of cavity is properly controlled, the debonding can grow gradually.

1. Introduction

When a rubber cylinder is well confined on both edges, a comparatively small tension force will lead to reversible cavity or irreversible crack within the cylinder [1]. This phenomenon is called cavitation instability, resulting from a negative hydrostatic pressure in the incompressible rubber cylinder. Similar phenomenon was found in elastomeric composites. Visible void appeared in the layers of silicone rubber which was bounded between steel spheres or steel cylinders [2]. Cavitation can also be found in Newtonian fluid and polymeric-based soft materials, which have intermediate mechanical properties between stiff rubber and Newtonian fluid [3]. In addition to macroscale cavities, we could also see nanoscale cavitation, because nanoscale rubber domain was created between aggregated nanoparticles, which could lead to macroscopic cracks [4].

For a spherical cavity subjected to internal hydraulic pressure in soft solids, an analytical solution was proposed and agreed well with the experiments [1]. As the pressure increases to a critical value P_c, given by $5E/6$ where E is elasticity modulus, the cavity will grow without limit. Later, effect of surface tension was also considered, and critical pressure would increase to overcome resistance from surface energy[5]. In real experiments, cavity cannot expand without limit and it will transit to crack once energy release rate reached critical value of fracture. This transition was studied analytically and numerically[6], [7].

However, cavitation phenomenon is not always related to failure of structure or undesiring outcome. In natural world, humidity change induces cavitation instability in fern sporangium, which helps to eject seeds at high speed [8]. A method called cavitation rheology technique (CRT) was also developed to determine local modulus of materials based on previous theory[9]–[11]. Single cavity was introduced at the tip of syringe needle and grew rapidly as

pressure increased to 5*E*/6. This snap-through instability was accompanied by a decrease of pressure and then material properties was calculated. This snap-through instability of a bubble in an elastomer was studied analytically, and both surface tension and stretch limitation of the elastomer was taken into consideration in the model [12]. Also, CRT method shows great potential in measuring heterogeneous materials and biological tissues *in vivo* [13].

In CRT test, stress state around needle tip is not stress free and we found retraction of needle can reduce stress, but meantime non-spherical cavity would be induced. Previously several works about the non-spherical cavitation were made. Expansion of an isolated ellipsoidal cavity in linearly viscous solid and rigid-perfectly plastic was studied [14]. A spherical cavity subjected to unequal far-field stress would not expand homogenously, instead the spherical cavity would expand and deform to ellipsoidal one [15]. Analytical calculation, numerical analysis and experiments were taken to study the expansion of a long cylindrical cavity through a Neo-Hookean solid, and peristaltic elastic instability showed up in this work[16].

However, according to our knowledge, no report about non-spherical cavitation introduced by CRT is available. In this thesis, first we are going to demonstrate for a soft solid, shape of initial cavity does influence expansion and corresponding critical pressure by finite element (FE) analysis. Then research about needle induced tubular cavitation in CRT is conducted. Effect of tubular geometry and surface tension are both taken into consideration with the help of ABAQUS. Localized bulging and debonding between needle and elastomer are discussed too. These works may give more insight into the CRT test.

2. Ellipsoidal cavitation in infinite large elastomer

2.1 Finite element model

Numerical analysis about ellipsoidal cavitation within an infinite large elastomer is studied. The schematic of our model is shown in Figure 2.1. The problem is simplified to 2D case by using axisymmetric model. *A* and *B* are initial horizontal and vertical semiaxis length of ellipse respectively. Cavity is subjected to interior homogenous pressure *P*. Circular shape is adopted for the soft solid to create better mesh for finite element model. The radius of circle *R* is much larger than the characteristic length of the void, so the elastomer can be viewed as infinite large one.

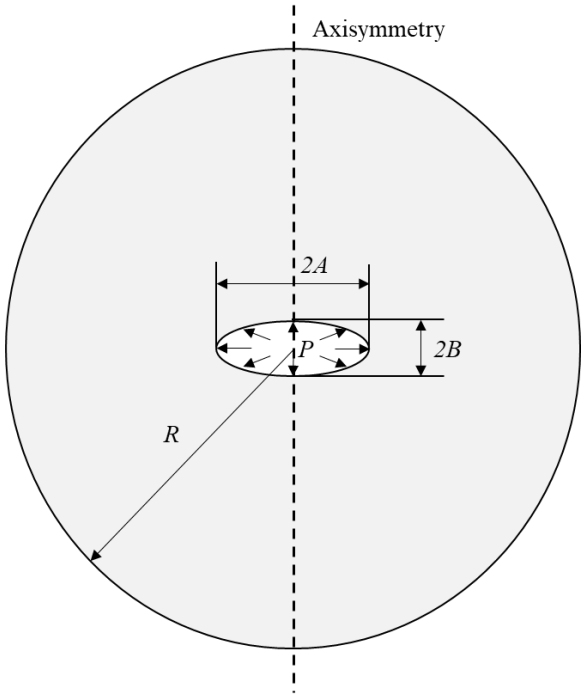

Figure 2.1: Schematic of ellipsoidal cavitation within an infinite large elastomer

ABAQUS standard is used to conduct quasi-static simulations of cavitation. Figure 2.2 shows five FE models with different *A*/*B* ratios, from cylinder-like cavity to penny-shape crack. Total numbers of element are 9947, 11544, 12848, 10788 and 9695 respectively. CAX4H

element is used for the analysis and mesh is greatly refined near the cavity. Neo-Hookean hyperelasticity model is used and elastomer is set to be incompressible.

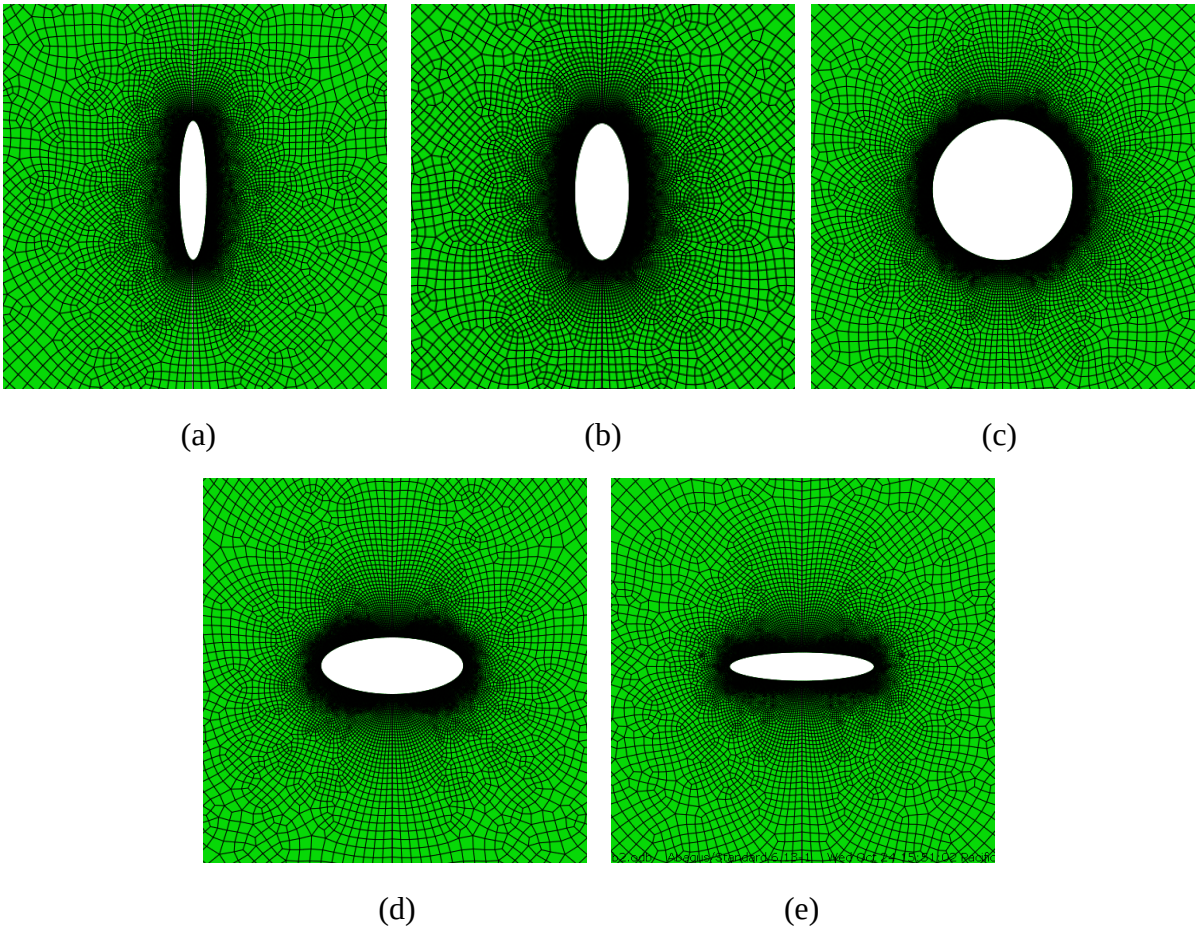

(a) (b) (c)

(d) (e)

Figure 2.2: Finite element mesh configurations of ellipsoidal cavitation. (a) A/B=2/10. (b) A/B=4/10. (c) A/B=10/10. (d) A/B=10/4. (e) A/B=10/2

2.2 Results and discussion

We introduced a geometry parameter $r=B/A$, where B and A are defined same as before. When r is much larger than 1, the cavity is close to a cylinder, and as r decreases the geometry of cavity will become a sphere (r=1) and then a penny-shape crack (r=0). First based on previous work[14], we get analytical solutions of ellipsoidal cavitation in an incompressible linear elastic material with Young's modulus E. With pressure P applied on the surface of cavity,

the lengths of horizontal semi axis *a* and vertical semi axis *b* at deformed configuration are as follows:

$$a = \frac{r^2\left(2+\alpha-3\beta\right)}{6\alpha\left(2r^2+\beta\left(1-r^2\right)\right)}\frac{PA}{E} \tag{2-1}$$

$$b = \frac{r^2\alpha}{6\alpha\left(2r^2+\beta\left(1-r^2\right)\right)}\frac{PB}{E} \tag{2-2}$$

in which *r* is geometry parameter, α and β are two values related to geometry parameter *r* . The expressions are given as:

$$\beta = \begin{cases} r\left(1-r^2\right)^{-3/2}\left(\cos^{-1} r - r\left(1-r^2\right)^{1/2}\right), r<1 \\ 2/3, r=1 \\ r\left(r^2-1\right)^{-3/2}\left(r\left(r^2-1\right)^{1/2} - \cosh^{-1} r\right), r>1 \end{cases} \tag{2-3}$$

$$\alpha = \begin{cases} 2/5, r=1 \\ r^2\left(r^2-1\right)^{-1}\left(3\beta-2\right), else \end{cases} \tag{2-4}$$

The geometry *A*/*B*=10/4 is used to do a comparison between Neo-Hookean material and linear elastic one, as shown in Figure 2.3. Results of Neo-Hookean material with shear modulus μ are calculated by FEM. When material is incompressible, shear modulus μ equals to 3 times of elastic modulus *E*. From the plot we can tell linear elasticity shows a good approximation when deformation is relatively small, but for large deformation case it is quite different from Neo-Hookean material. Usually cavitation phenomenon is studied in highly nonlinear material like rubber or hydrogel at large deformation, and analytical method is limited to some special cases. Instead, FEM is a powerful tool to do numerical analysis, and our work next are all conducted with the help of FEM software ABAQUS.

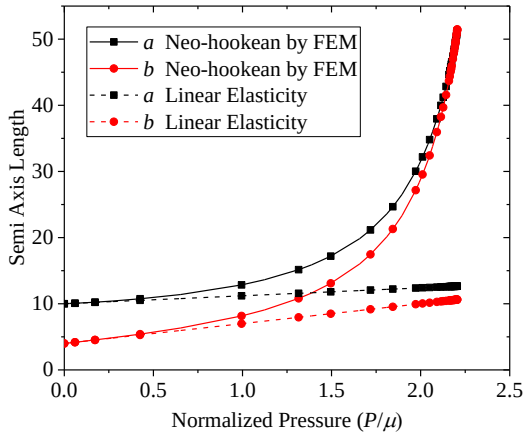

Figure 2.3: Deformed semi axis lengths *a* and *b* vs normalized pressure. Comparison between Neo-Hookean material by FEM and linear elastic material by analytical analysis is made.

The influence of initial cavity geometry to cavity expansion is studied. Figure 2.4 (a) shows that for models with various initial *A*/*B* ratios, the cavity shape tends to become spherical when pressure increases. As illustrated in Figure 2.4 (b), the pressure-volume curves possess similar trend. At beginning pressure increase will not lead to fast cavity growth but when pressure gets close to critical value, the volume increase can be obvious, and the slenderer the initial shape is, the larger the asymptotic pressure is.

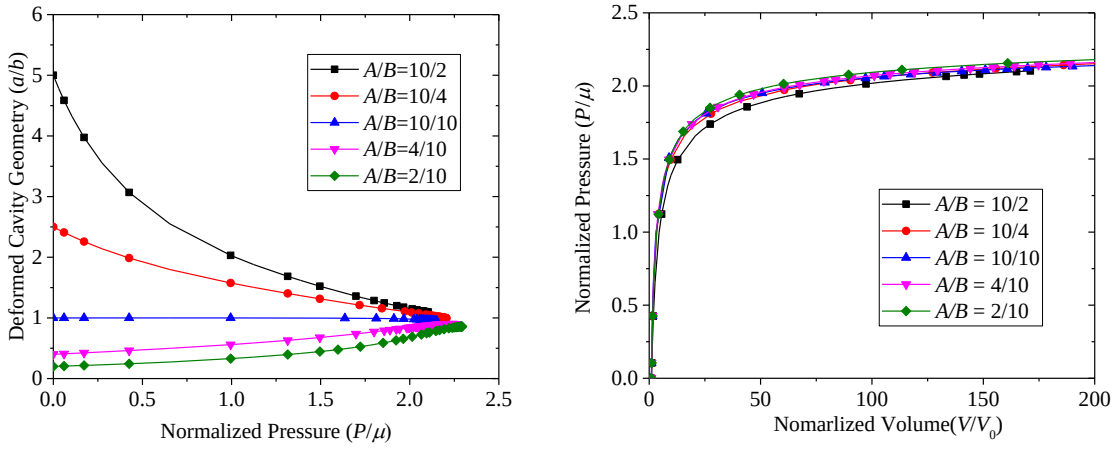

(a) (b)

Figure 2.4: Influence of initial cavity geometry to ellipsoidal cavitation. (a) *a*/*b* ratio vs normalized pressure for cavities with different initial shapes. (b) Normalized pressure vs volume with respect to different cavities from cylinder to penny-shape one

From calculations above we can tell geometry of the cavity play a role in the cavitation phenomenon. In real experiment void shape is more important as stress concentration will lead to crack propagation.

3. Needle induced tubular cavitation

Cavitation rheology technique (CRT) involves sensing the pressure of a cavity within a soft material. Main components of CRT are a syringe pump, pressure sensor, microscope and personal computer [9]. However, the gel around the needle is compressed and not stress free, which may influence the precision of results. We find stress is reduced if needle is retracted, but then a tubular cavity is induced. In this chapter, needle induced tubular cavitation is discussed with respect to influence of retraction and surface tension, localized bulging of tubular cavity and debonding between needle and elastomer.

3.1 Influence of needle retraction and surface tension

After retracting needle with a certain distance, a tubular cavity is created. It is intuitive to study the influence of cavity geometry, namely the retraction distance, to its expansion. The schematic of FE model is shown in Figure 3.1 (a) and OA and AC are radius and length of the tubular cavity. Axisymmetric model is used to reduce the complexity of calculation as shown in Figure 3.1 (b) and the mesh around cavity is greatly refined as shown in Figure 3.1 (c). Four models with AC/AO = 1, 3, 5 and 7 are used to study influence of retraction distance. Total numbers of element are 76046, 82280, 96892 and 107064 respectively. CAX4H element with Neo-Hookean material property are assigned to the model.

Figure 3.2 shows normalized pressure-volume relationship with respect to different AC/AO ratios. The trend of curves is close to spherical cavitation. The pressure-volume relationship is monotonic, and when pressure reaches critical value the cavity can grow rapidly,

but asymptotic pressure of tubular cavitation is higher than spherical cavitation and critical pressure further increases with decreasing of tubular cavity length. This agrees with results in Chapter 2 that a slim ellipsoidal cavity needs higher pressure to expand compared with spherical one.

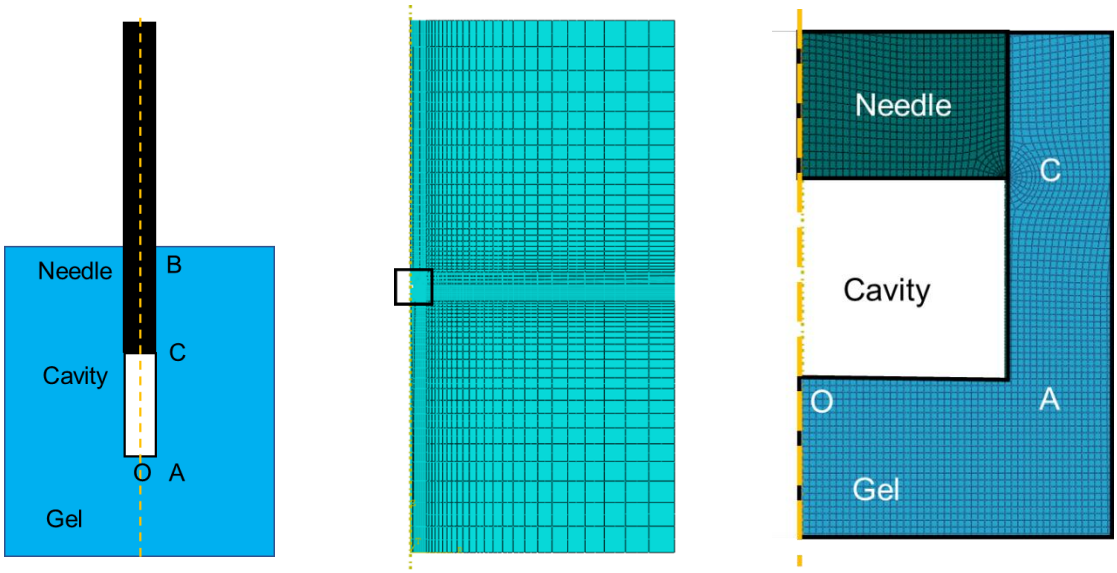

(a) (b) (c)

Figure 3.1: Schematic and FE model of needle induced tubular cavitation. (a) Schematic of tubular cavity in elastomer induced by needle retraction. (b) Axisymmetric FE model, and mesh is greatly refined around cavity. (c) Mesh configuration near tubular cavity

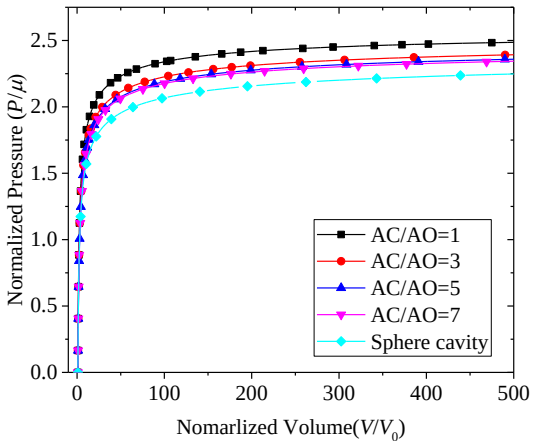

Figure 3.2: Pressure vs volume with respect to different retraction distances for tubular cavitation. AO and AC are radius and height of tubular cavity.

Previous work [17] provides us a user-defined subroutine to include effect of surface tension to ABAQUS standard calculation. Neo-Hookean and Gent materials are available for the user-define element. Model with AC/AO is set to be 5, to discuss the effect of surface tension. The first step of FE analysis is to increase surface tension γ from 0 to a given value, and during the second analysis step γ is kept as a constant while pressure is applied gradually. As shown in Figure 3.3, with larger surface tension, higher pressure is required for the cavity to expand, which is straightforward that surface tension will increase resistance to cavity growth and higher pressure is needed to overcome the effect of surface energy.

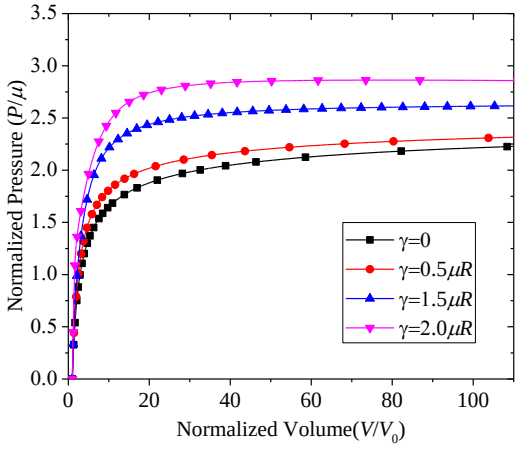

Figure 3.3: Effect of surface tension γ to tubular cavitation. Model with AC/AO=5 is used. μ is shear modulus of Neo-Hookean material and R is the radius of tubular cavity.

3.2 Localized bulging along long tubular cavity

In experiment, we find localized bulging phenomenon happens a lot when retraction distance is relatively large and usually initial defect is observed first at bulging area. Initial defect and surface tension are two possible reasons come to mind.

To simplify this problem, we treat the long tubular cavity in experiment as infinite long and Figure 3.4 (a) illustrate the schematic of our model. By taking advantage of symmetry, quarter model, a rectangle part ABCD, is used as FE model as shown in Figure 3.4 (b). Two

characteristic nodes, one at the center and one away from center, are picked to study the localized bulging phenomenon. As the length and thickness of the elastomer are much larger than the radius of tubular cavity, this model can simulate expansion of an infinite long tubular cavity within an infinite large elastomer.

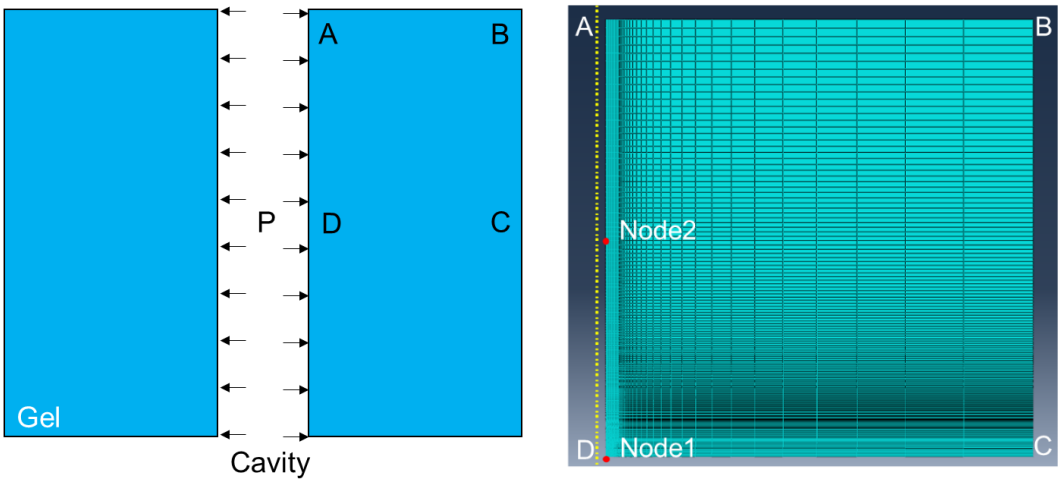

(a) (b)

Figure 3.4: Schematic and FE model of infinite long tubular cavity in an elastomer. (a) Quarter model ABCD is used for FEM. (b) FE model, mesh is greatly refined near cavity. Node 1 and 2 are two characteristic nodes at the center and away from center respectively

Expansion ratio λ, defined as deformed cavity radius r divided by undeformed cavity radius R, is adopted to study the deformation of cavity. First, only the effect of surface tension is considered, and no initial defect is introduced at center of the cavity. As shown in Figure 3.5 (a), expansion ratio is smaller than one after surface tension is applied, which means cavity shrink first to low down the area of cavity. Then cavity expands with the increase of inner pressure. As surface tension increases, higher pressure is needed to overcome the resistance due to surface energy. One interesting phenomenon is that the curve become non-monotonic when surface tension γ is greater than $2\mu R$, where μ is shear modulus of material and R is initial radius

of tubular cavity. Thus Snap-through instability will happen because lower pressure is required for cavity to expand when critical pressure is reached.

However, this instability is homogenous along the whole cavity but in the experiment, we can always see localized bulging and usually defect is observed first before the bulging, so we introduce a small defect at the center of FE model, in which Node 1 locates. Expansion ratios at of two characteristic nodes are compared in Figure 3.5 (b) with different surface tension. From the plot we know when surface tension γ is below critical value $2\mu R$, expansion ratios at the defect and away from the defect are the same, which means there is no localized bulging. When pressure-expansion ratio relationship is non-monotonic, namely $\gamma/\mu R$ is higher than 2, localized bulging shows up as Figure 3.6 (a). The cavity will increase homogenously first and then elastomer at defect (Node1) will bulge out while the radius away from defect (Node2) will decrease a little bit, but expansion will become homogenous again as pressure further increases, as illustrated in Figure 3.6 (b). And with higher surface tension, the cavity bulges out more.

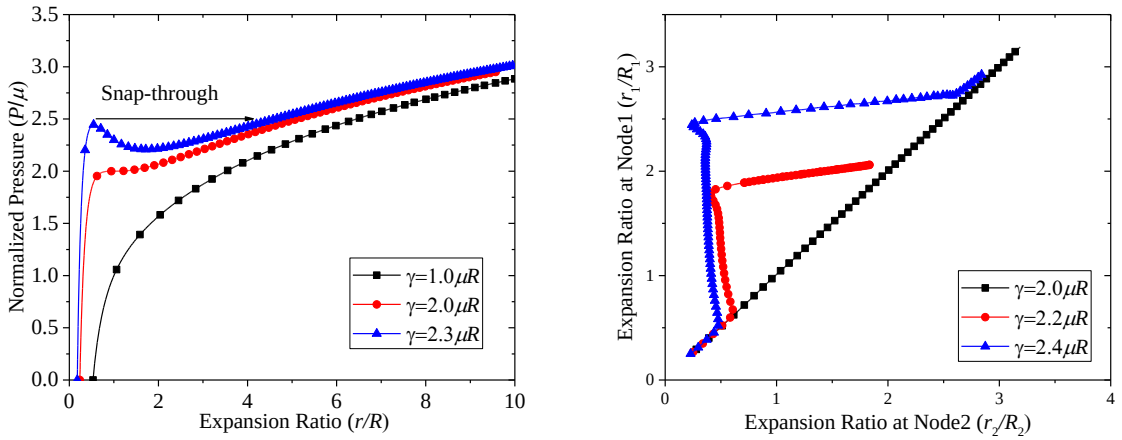

(a) (b)

Figure 3.5: Comparison of long tubular cavitation between model without defect and model with initial defect. (a) Pressure-expansion ratio relationship of model with no defect. (b) r_1/R_1 vs r_2/R_2 of model with defect, subscript 1 and 2 correspond to expansion ratios at node 1 and node 2. r and R are radii at deformed configuration and undeformed configuration.

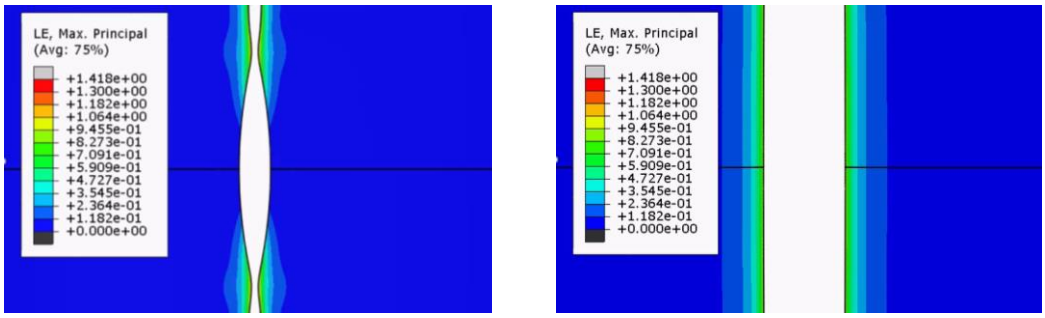

(a) (b)

Figure 3.6: Max principal strain contours of long tubular cavitation. (a) Localized bulging at the defect. (b) Recovery to homogenous expansion along the tubular cavity

3.3 Debonding between needle and elastomer

For a finite long, tubular cavitation as shown in Figure 3.7 (a), singular font shows up when inner pressure increases because debonding between needle and elastomer is suppressed for previous model. However, in real experiment, the interface can not sustain infinite large shear traction between needle and elastomer, so next debonding problem is studied for the needle induced tubular cavitation. The schematic of FE model is illustrated in Figure 3.7 (b). Same as previous model OA is the radius of tubular cavity, AC is the length of tubular cavity and a debonding, BC, between needle and elastomer is included.

Energy release rate is used to decide whether a crack tip will grow or not. It is defined as energy dissipation per new formed fracture surface during crack propagation. For the FE method, energy release rate at crack tip is calculated by J integral in ABAQUS. Path independence of J integrals is checked to validate convergence of J integral. Also, to evaluate the reliability of J integral, we also use two FE models with close crack length to calculate energy release rate at crack tip, which is based on the definition of energy release rate. The results by two method are compared as shown in Figure 3.9, indicating the reliability of J integral exported from ABAQUS.

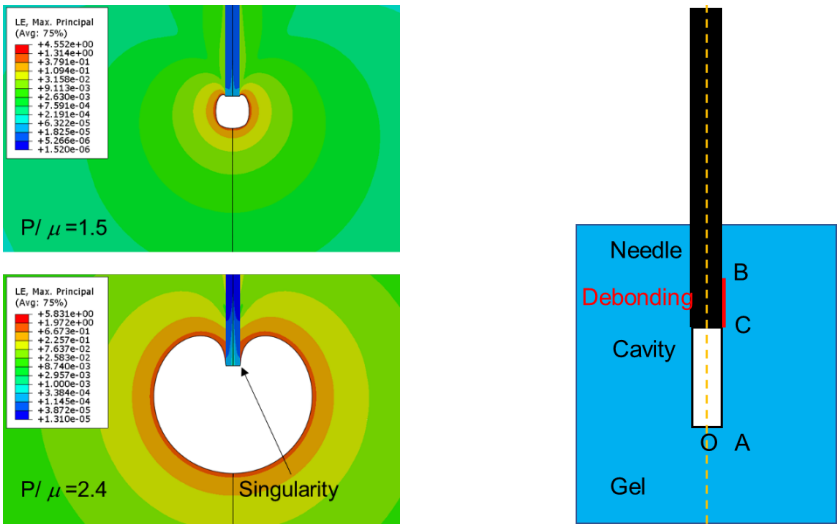

(a) (b)

Figure 3.7: (a) Max principal strain contours of model without debonding at P/μ=1.5 and 2.4. (b) Schematic of tubular cavitation model with debonding. OA is the radius of tubular cavity, AC is the length of tubular cavity and BC is debonding length between elastomer and needle.

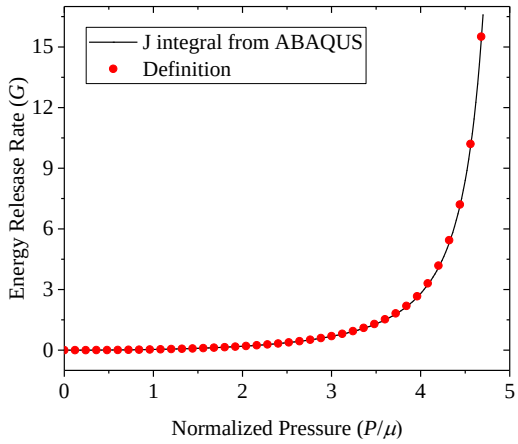

Figure 3.8: Reliability validation of energy release rate by J integral

First, we calculate energy release rate-pressure relationship for model without debonding with respect to different retraction distance AC/AO where AC and AO are retraction distance and initial cavity radius. As illustrated in Figure 3.9 (a). The energy release rate increases rapidly as pressure reaches asymptotic value and detachment starts because critical energy release rate for the crack to propagate is reached. It becomes easier to debond with

increasing debonding distance, but the energy release rate vs pressure curves converge as retraction distance further increases.

Then we set the retraction distance as a constant, namely AC/CO=5, and variate debonding length BC/AO from 0.5 to 5. The energy release rate-pressure relationship is shown in Figure 3.9 (b). Still, energy release rate increases rapidly when pressure gets close to asymptotic value. For a given pressure, energy release rate slightly decreases as debonding becomes longer and this is further illustrated in Figure 3.10 (a). This means when pressure reaches a critical value there would be a fast debonding process. For the volume control cavitation, the energy release rate decreases obviously as crack propagates for a given cavity volume, which means debonding will not continue until cavity volume further increases. This volume control method is hard to realize in experiment because we usually see rapid volume growth at the end of experiment as pressure then is really close to asymptotic pressure.

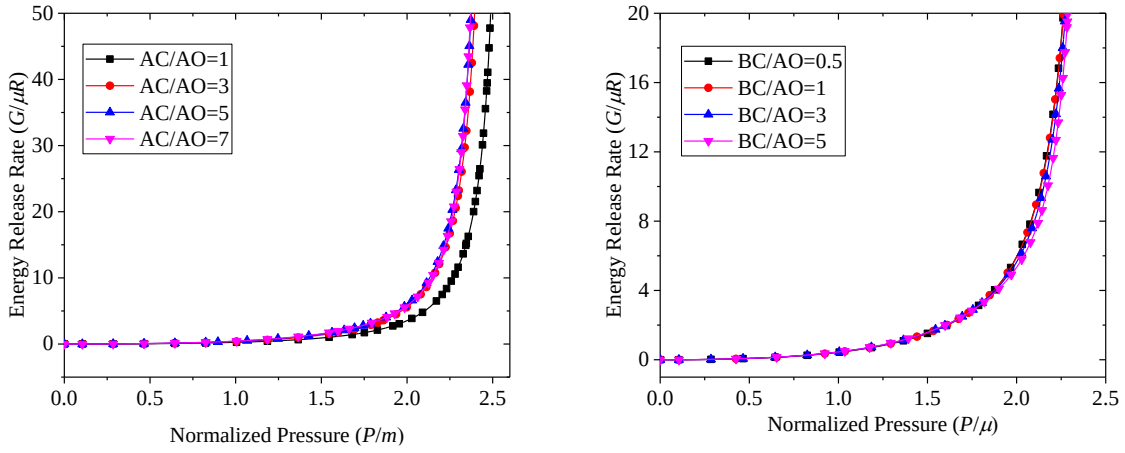

(a) (b)

Figure 3.9: Energy release rate vs normalized pressure for model with and without initial debonding. (a) Model without debonding, different retraction distances are considered. (b) Model with debonding, different crack lengths are considered

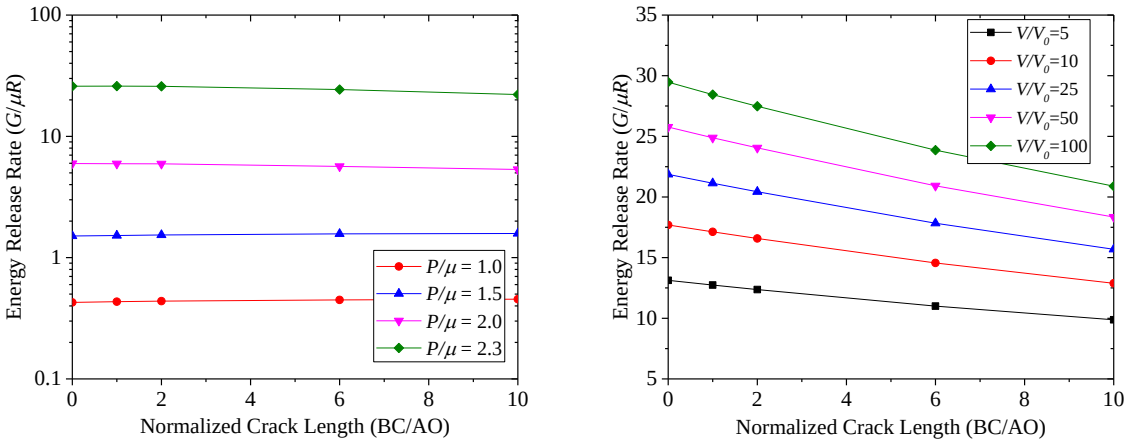

(a) (b)

Figure 3.10: Energy release rate vs normalized crack length at a given pressure or volume. (a) Pressure is controlled as a constant. (b) Volume is controlled as a constant.

4. Conclusion

In this thesis, we consider the mechanical response of non-spherical cavity to inner pressure. We find that geometry mainly influences the asymptotic pressure at which void expands rapidly. For ellipsoidal cavitation with various geometries, from oblate one to prolate one, it shows that prolate cavity needs higher asymptotic pressure than oblate one and spherical one has intermediate asymptotic pressure.

As for needle induced retraction, longer tubular cavity has comparatively lower critical pressure, and surface tension will increase the critical pressure. Also, localized bulging of tubular cavity happens at the defect when surface tension is large enough. We notice the mode of bulging by finite element method is different from experiment, one possible explain is that crack propagation also happens around defect during experiment. Debonding between soft solid and rigid needle is studies. We find it is fast for elastomer and needle to debond when pressure is close to the critical pressure, but if volume of cavity is properly controller, the debonding can grow gradually. However, volume control method is hard to realize in real experiment because we usually see rapid volume growth at the end of experiment as pressure then is really close to asymptotic pressure.

References

[1] A. N. Gent and P. B. Lindley, "Internal Rupture of Bonded Rubber Cylinders in Tension," *Proc. R. Soc. A Math. Phys. Eng. Sci.*, vol. 249, no. 1257, pp. 195–205, Jan. 1959.

[2] K. Cho and A. N. Gent, "Cavitation in model elastomeric composites," *J. Mater. Sci.*, vol. 23, no. 1, pp. 141–144, 1988.

[3] A. Chiche, J. Dollhofer, and C. Creton, "Cavity growth in soft adhesives," *Eur. Phys. J. E*, vol. 17, no. 4, pp. 389–401, 2005.

[4] H. Zhang, A. K. Scholz, J. De Crevoisier, F. Vion-Loisel, G. Besnard, A. Hexemer, H. R. Brown, E.J. Kramer, C.Creton, "Nanocavitation in carbon black filled styrene-butadiene rubber under tension detected by real time small angle X-ray scattering," *Macromolecules*, vol. 45, no. 3, pp. 1529–1543, 2012.

[5] A. N. Gent and D. A. Tompkins, "Surface Energy Effects for Small Holes or Particles in Elastomers," *J. Polym. Sci. Part A-2*, vol. 7, pp. 1483–1488, 1969.

[6] A. N. Gent and C. Wang, "Fracture mechanics and cavitation in rubber-like solids," *J. Mater. Sci.*, vol. 26, no. 12, pp. 3392–3395, 1991.

[7] J. Kang, C. Wang, and S. Cai, "Cavitation to fracture transition in a soft solid," *Soft Matter*, vol. 13, no. 37, pp. 6372–6376, 2017.

[8] J. Kang, K. Li, H. Tan, C. Wang, and S. Cai, "Mechanics modelling of fern cavitation catapult," *J. Appl. Phys.*, vol. 122, no. 22, 2017.

[9] J. A. Zimberlin, N. Sanabria-Delong, G. N. Tew, and A. J. Crosby, "Cavitation rheology for soft materials," *Soft Matter*, vol. 3, no. 6, pp. 763–767, 2007.

[10] S. Kundu and A. J. Crosby, "Cavitation and fracture behavior of polyacrylamide hydrogels," *Soft Matter*, vol. 5, no. 20, pp. 3963–3968, 2009.

[11] A. Delbos, J. Cui, S. Fakhouri, and A. J. Crosby, "Cavity growth in a triblock copolymer polymer gel," *Soft Matter*, vol. 8, no. 31, pp. 8204–8208, 2012.

[12] J. Zhu, T. Li, S. Cai, and Z. Suo, "Snap-through expansion of a gas bubble in an elastomer," *J. Adhes.*, vol. 87, no. 5, pp. 466–481, 2011.

[13] J. A. Zimberlin, J. J. McManus, and A. J. Crosby, "Cavitation rheology of the vitreous: Mechanical properties of biological tissue," *Soft Matter*, vol. 6, no. 15, pp. 3632–3635, 2010.

[14] L. Banks-Sills and B. Budiansky, "On void collapse in viscous solids," *Mechanics of Materials*, vol. 1, no. 3. pp. 209–218, 1982.

[15] Y. W. Chang, A. N. Gent, and J. Padovan, “Expansion of a cavity in a rubber block under unequal stresses,” Kluwer Academic Publishers, 1993.

[16] N. Cheewaruangroj, K. Leonavicius, S. Srinivas, and J. S. Biggins, “Peristaltic elastic instability in an inflated cylindrical channel,” no. 1, pp. 1–6, 2018.

[17] D. L. Henann and K. Bertoldi, “Modeling of elasto-capillary phenomena,” *Soft Matter*, vol. 10, no. 5, pp. 709–717, 2014.